Aspects of the Non-Zonal Transition

M.J. Pueschel[1], P.W. Terry[1], and D.R. Hatch[2]

[1] *Department of Physics, University of Wisconsin-Madison, Madison, Wisconsin 53706, USA*

[2] *Institute for Fusion Studies, University of Texas at Austin, Austin, Texas 78712, USA*

Abstract

The non-zonal transition, a process which can bring about very large heat fluxes in gyrokinetic simulations, occurs once a certain threshold plasma β is reached. This threshold is parameterized via a simulation database, yielding an expression estimating at what β a given system may approach the transition. Furthermore, the diffusive outward transport of a heat blob in a temperature profile marginally stable with respect to the non-zonal transition is discussed: the resulting transport timescale corresponds to the geometric mean of the underlying turbulent transport timescale and the linear instability growth time, thus demonstrating that the non-zonal transition provides a mechanism for very fast heat dissipation.

I. INTRODUCTION

Recently, the non-zonal transition (NZT) has been proposed as an explanation of the high-β runaway [1, 2]. The latter occurs in gyrokinetic simulations of ion-temperature-gradient-driven (ITG) turbulence, where it causes turbulent amplitudes and transport levels to grow to extremely large values once a certain electron normalized plasma pressure β is exceeded. As it had been unclear whether this effect was a result of shortcomings of the available gyrokinetic codes (e.g., problems arising from numerical algorithms), very few prior publications exist discussing this phenomenon [3, 4].

ITG modes are known to saturate via energy transfer to zonal flows [5], which are poloidally and toroidally constant electrostatic perturbations $\Phi_{\mathrm{ZF}} = \Phi_{\mathrm{ZF}}(x)$, where x is the radial coordinate. Zonal flows act as a barrier for radial heat and particle transport, which is why heat flux levels in ITG turbulence are significantly lower than renormalized fluxes of electron-temperature-gradient-driven turbulence [6] for equivalent parameter regimes. If some process is able to prevent ITG saturation via zonal flows, the expected result will be that the quasi-stationary turbulent state will be achieved only at excessively large amplitudes and fluxes.

This is exactly what occurs during the NZT: the zonal flows are depleted, thus no longer saturating the ITG mode at low amplitude. The depletion is a consequence of parallel electron motion in strongly stochastic magnetic fields. The resulting radial motion allows them to cross the radial barrier as which the zonal flow acts, thereby contributing to a current that reduces the radial gradient in the electrostatic potential corresponding to the zonal flow [8]. If this diminishing action depletes the zonal flow more quickly than the secondary instability mechanism [7] of the ITG mode is able to replenish it, the system can no longer rely on zonal flow activity to regulate its turbulent dynamics.

The reason why the NZT occurs very suddenly has been traced back to a sudden increase in magnetic stochasticity [9], caused by the decorrelation of the odd-parity component $B_x^{\mathrm{odd}}(z) = (B_x(z) - B_x(-z))/2$ of the radial magnetic field perturbation, with the parallel coordinate denoted by z. While usually not able to break magnetic flux surfaces, B_x^{odd} may contribute to the stochasticity of a field line if the latter, integrated from the inboard to the outboard mid-plane, decorrelates from the (perturbed) field: in this case, the path back from the outboard to the inboard side is statistically independent from the first half poloidal

turn, and the field line will, in general, not return to its original radial position. In other words, increasing β and therefore B_x^{odd} continuously displaces a field line at the outboard side from its radial position at the inboard side by an increasing amount, only to find its way back to the original inboard position by completing its poloidal turn. If, however, the displacement exceeds the correlation length of B_x at the outboard side, the second half of its journey will lead it to a completely different position on the inboard. Therefore, an electron following this field line will now experience a radial displacement after one poloidal turn, leading to a radial current which, as described above, influences the zonal flow. It is to be stressed that in this process, electrons are removed from the original, unperturbed flux surface, not from their respective perturbed field lines. More details on the NZT and on field line decorrelation may be found in Refs. [1, 2].

In this paper, two additional aspects of the NZT are studied. First, a database of various gyrokinetic simulations is utilized to provide a simple way of estimating at what $\beta_{\mathrm{crit}}^{\mathrm{NZT}}$ the NZT may occur for a given parameter set. Then, the impact of crossing this threshold on the transport rate of a heat blob in a fusion device is examined.

II. A SIMPLE PARAMETERIZATION OF THE NZT THRESHOLD

To develop a better intuition about the NZT threshold $\beta_{\mathrm{crit}}^{\mathrm{NZT}}$, use is made of a database of radially local electromagnetic gyrokinetic turbulence simulations which was originally created to parameterize fast particle diffusion; for more details on the database and the constituting simulations, see Ref. [10]. Here, the database is used to empirically derive expressions for the two key parameters determining NZT onset: the half-turn radial displacement $\Delta r_{1/2}$ of magnetic field lines and the radial correlation length λ_{Bxx} of the radial magnetic field perturbation. The intersection of these two quantities defines the onset of the enhanced magnetic stochasticity described above.

For the present purpose, in order to estimate $\Delta r_{1/2}$, it is helpful to first obtain an expression for B_x. With the results of Ref. [10] in mind, an appropriate choice is to replace the magnetic field fluctuation with $\alpha_B \chi_{\mathrm{eff}}^{1/2} \beta / \beta_{\mathrm{crit}}^{\mathrm{KBM}}$, where χ_{eff} is the sum of the ion and electron heat diffusivity (in gyro-Bohm units with normalization to the major radius R_0) and α_B is a scaling factor which turns out to be equal to 0.15: as illustrated in Fig. 1, this constitutes a relatively good description of B_x. There also exists a physical rationale for

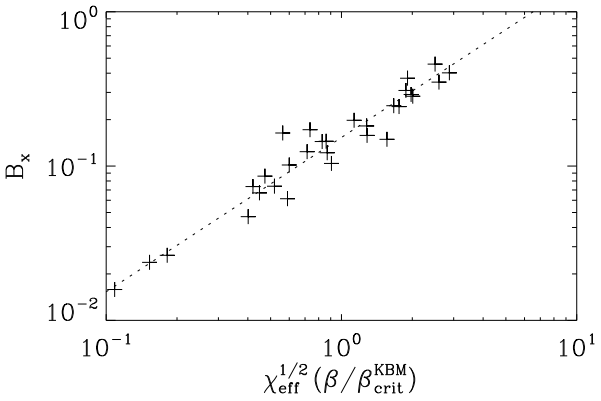

FIG. 1. Scatter plot of various gyrokinetic simulations, showing B_x in units of $B_0\rho_{\rm s}/R_0$ as a function of $\chi_{\rm eff}^{1/2}\beta/\beta_{\rm crit}^{\rm KBM}$; here, the heat diffusivity has units of $c_{\rm s}\rho_{\rm s}^2/R_0$. The dotted fit corresponds to a slope of $\alpha_B = 0.15$.

this substitution: $\chi_{\rm eff}$ relates directly to the (squared) turbulent fluctuation level; whereas $\beta/\beta_{\rm crit}$ tends to govern the ratio of the (averaged) amplitudes of the electrostatic to those of the electromagnetic fluctuations (see also Ref. [11]).

Translating B_x into $\Delta r_{1/2}$ can be achieved through simple integration as follows:

$$\Delta r_{1/2} = \int_{-\pi q_0 R_0}^{0} {\rm d}z\, \frac{B_x(z)}{B_0} = \frac{\eta_B \pi q_0 R_0 \langle B_x \rangle_{\rm rms}}{B_0}\ . \tag{1}$$

In the last step, the half-turn average is replaced by the full-turn root-mean-square average, along with a scaling factor η_B. The variation of the background field B_0 along z is assumed to be small. The quantity B_x plotted in Fig. 1 is also a root-mean-square. The introduction of η_B becomes necessary because, in general, the half-turn average is not identical to the root-mean-square of B_x—for instance, if both positive and negative values of B_x occur within the first half turn, they will not cancel in the root-mean-square. To obtain a generally applicable value for η_B, its average is taken for the three parameter cases – the Cyclone Base Case [12] (CBC), the GA standard case (see, e.g., Ref. [4]), and the trapped electron mode (TEM) case in Ref. [13] – described in Ref. [2], yielding $(2.44 + 2.16 + 2.20)/3 = 2.3$, which shall be used to estimate $\Delta r_{1/2}$ below. The fact that all three values are very similar serves as an indication that this relation may be of more general relevance.

The other parameter necessary to predict the NZT threshold is the radial correlation length of B_x, denoted by λ_{Bxx}. While clearly, more intricate parameterizations of this quantity can be envisioned, Fig. 2 demonstrates that simply taking λ_{Bxx} to be a constant

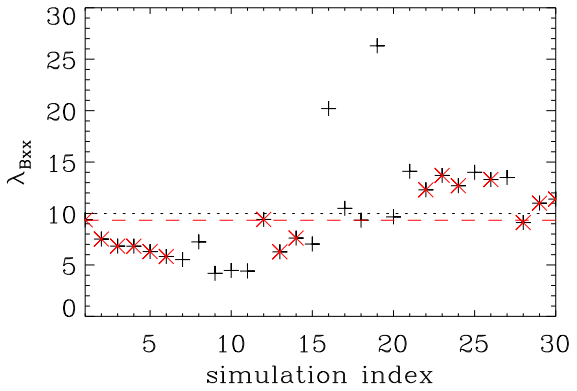

FIG. 2. (Color online) Scatter plot (black +'s) of various gyrokinetic simulations, showing λ_{Bxx} in units of ρ_s without any parametric dependence. The mean (black dotted line) marks $\bar{\lambda}_{Bxx} = 10.0$. Selecting only simulations which exhibit ITG turbulence (red ×'s) yields a slightly lower average $\bar{\lambda}^{\mathrm{ITG}}_{Bxx} = 9.3$ (red dashed line).

is not an unreasonable assumption, yielding a value of 9.3 in units of ρ_s for simulations with ITG characteristics (or 10.0 when including simulations with TEM or microtearing turbulence).

Setting the correlation length equal to the half-turn displacement in order to obtain $\beta^{\mathrm{NZT}}_{\mathrm{crit}}$ yields

$$\lambda_{Bxx} = \Delta r_{1/2} = \pi q_0 R_0 \alpha_B \eta_B \chi_{\mathrm{eff}}^{1/2} \frac{\beta^{\mathrm{NZT}}_{\mathrm{crit}}}{\beta^{\mathrm{KBM}}_{\mathrm{crit}}} \ . \tag{2}$$

With the values for α_B, η_B, and λ_{Bxx}, this expression becomes

$$\frac{\beta^{\mathrm{NZT}}_{\mathrm{crit}}}{\beta^{\mathrm{KBM}}_{\mathrm{crit}}} \approx \frac{8.6}{q_0} \chi_{\mathrm{eff}}^{-1/2} \ . \tag{3}$$

This result, its derivation having involved fits to (moderately) scattered data points, is not meant to be used to obtain precise predictions, but rather for a simple initial estimate of whether a particular case may be prone to an NZT. More precise answers require nonlinear simulations to obtain $\Delta r_{1/2}$ and λ_{Bxx} directly. However, it is now possible to get a sense of whether a given parameter set may be close to an NZT, simply by using a heat diffusivity estimate from, e.g., quasilinear models.

This estimate can now be tested against simulation data. For all aforementioned cases (the CBC, GA standard, and TEM case), the predicted NZT threshold lies within approximately 40% of the respective measured value. This illustrates the above statement that Eq. (3) provides a reasonable estimate. Moreover, the deviations are consistent with

the scatter in Fig. 2; note that no GA standard case data is included in the database in Ref. [10]. As a consequence, a more encompassing model for predicting the correlation length – which is beyond the scope of this work – can be expected to result in improved accuracy for predictions of $\beta_{\rm crit}^{\rm NZT}$.

Equation (3) also offers an explanation as to why $\beta_{\rm crit}^{\rm NZT}$ is more sensitive to the background temperature gradient $\omega_{Tj} = (\partial T/\partial r)R_0/T$ of species j and the density gradient $\omega_n = (\partial n/\partial r)R_0/n$ than the KBM threshold $\beta_{\rm crit}^{\rm KBM} \sim (\omega_{Tj} + \omega_n)^{-1}$. In quasilinear models, the turbulent heat diffusivity χ is assumed to be proportional to the linear growth rate γ. In turn, a critical gradient $\omega_{T,\rm crit}$ tends to exist, below which $\gamma \leq 0$ and above which $\gamma \propto (\omega_T - \omega_{T,\rm crit})^{\xi}$, with typically $1/2 \lesssim \xi \lesssim 1$ for small $\omega_T - \omega_{T,\rm crit}$ [14, 15]. Inserting these simplified expressions into Eq. (3), one arrives at

$$\frac{\beta_{\rm crit}^{\rm NZT}}{\beta_{\rm crit}^{\rm KBM}} \propto (\omega_T - \omega_{T,\rm crit})^{-\xi/2} \ . \tag{4}$$

In other words, the normalized NZT critical β can be decreased by increasing the background gradients. This result agrees qualitatively with the gradient sensitivity studies reported in Ref. [1], and it suggests that if one is able to increase the background gradients sufficiently, one may force any system with relevant zonal flow activity to undergo an NZT.

Next, the focus is shifted to the dynamics of heat blobs in a temperature profile marginally stable to the NZT.

III. MARGINAL NZT HEAT BLOB PROPAGATION

In order to study the impact of the NZT mechanism on transport, it is instructive to look at the temporal evolution of a heat blob. This problem is adopted as a paradigm for a perturbative transport analysis associated with the deposition of a localized quantity of heat. If such a perturbation could be applied in a fusion experiment to a particular type of marginal temperature profile – e.g., with a localized heating source – it may be possible to confirm experimentally key aspects of the physics of the NZT. Whether the requisite marginal profile can be prepared experimentally is not addressed here. Our purpose is to develop, as a thought experiment, the measurable signatures that ensue. The exercise also serves to illustrate the physics of the NZT as they relate to transport. Figure 3 shows some temperature profile $T(r)$ on top of which a small perturbation $\tilde{T} \sim \epsilon^2 T$ is introduced, with

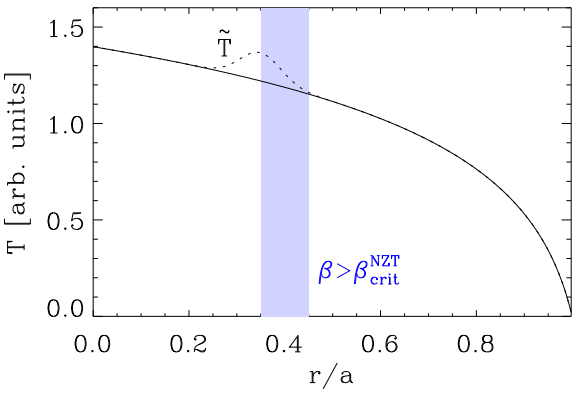

FIG. 3. (Color online) Temperature profile (solid line) with a small perturbation $\tilde{T}$ (dotted line). Throughout r, the unperturbed profile is postulated to be marginally stable with regard to the NZT. In the shaded region, however, the NZT threshold is exceeded due to the perturbation-enhanced gradient.

$\epsilon \ll 1$. This heat blob is spatially confined such that $\partial_x \tilde{T}$ may be of the same order as $\epsilon \partial_x T$—in other words, in part of the perturbed region, the temperature gradient is increased by a small increment. Furthermore, a number of assumptions are made:

1. The equilibrium can be characterized by a set of well-behaved, nested flux surfaces with flux label ψ.

2. The (unperturbed) temperature profile $T(\psi)$ is stationary in the presence of a heat source and heat transport.

3. Throughout the radial range, purely conductive heat transport is caused by ITG turbulence. For simplicity, it is assumed that heat is injected by a source at the magnetic axis and removed by a heat sink at the plasma surface.

4. At all radial positions, the unperturbed system is marginally stable with respect to the NZT threshold: $\beta(\psi) = \beta^{\mathrm{NZT}}_{\mathrm{crit}}(\psi)$.

The last condition is likely the most difficult to comply with in a realistic system, but as the aim of this exercise is to study the NZT impact, it is useful to assume global marginality. Note not only that a host of effects (e.g., edge physics) is neglected, but also that implicit assumptions regarding the density and/or magnetic field profile follow from the the last assumption, namely, the NZT marginality condition. Moreover, the assumptions imply that

the system is sufficiently far away from the ballooning threshold at all radial positions, and that the transport characteristics of the unperturbed profile are of ITG type.

Consider a diffusive temperature evolution equation

$$\frac{\partial T(\psi)}{\partial t} - \nabla \cdot \chi(\psi) \nabla T(\psi) = S \ , \tag{5}$$

where S is a source and $\chi(\psi)$ is the local heat flux of the ITG turbulence. If the profile is stationary, the diffusivity transports heat across each flux surface at the rate given by the source, yielding

$$n_0 \int \mathrm{d}S_\psi \, \chi(\psi) \nabla T \cdot \hat{\psi} = q_a \ , \tag{6}$$

where $q_a = \int n_0 S \, \mathrm{d}^3 x$ is the rate of thermal energy supplied by the source, $\hat{\psi}$ is the unit vector normal to the flux surface, $\mathrm{d}S_\psi$ is an element of area on the flux surface, and n_0 is the plasma density at the source. If A_ψ is the flux surface area and L_T is the temperature gradient scale length, the local diffusivity must satisfy

$$\chi(\psi) = \frac{q_a L_T(\psi)}{n_0 T(\psi) A_\psi} \ , \tag{7}$$

to maintain a stationary profile.

One may consider a perturbation to this steady profile, created by some radially localized deposition of heat, raising the temperature locally. The temperature perturbation will create a region (see Fig. 3) where the temperature gradient is enhanced; this, however, causes the NZT threshold to decrease. Additionally, a very small increase in $\beta \sim T + \tilde{T}$ occurs which can be neglected here due to the ϵ ordering. Because the unperturbed system is marginally stable at every radial position, the perturbed system becomes NZT-unstable locally. It needs to be stressed that enhanced ITG transport will also act on $\tilde{T}$, on a timescale of $\tilde{T}/q_a$. As will be shown *a posteriori*, NZT action occurs on a faster timescale.

Figure 4 illustrates in a simplified way how the turbulence is undergoing its non-zonal transition. At $t = 0$, the temperature gradient of the marginal system is increased, leading to an NZT once the zonal flow has decayed sufficiently, at $t = t_{\mathrm{ZF}}$. For simplicity, it is assumed that the turbulence is not affected by the zonal flow decay until the runaway phase. Exemplarily, in Fig. 5, actual turbulence undergoing an NZT is presented, for CBC parameters and at a β of 1.2%. While the specific temporal details of the turbulence obviously are far more irregular than in Fig. 4, the NZT-induced growth behavior is captured rather well by it. While it is not the aim of the present approach to capture encompassing transport

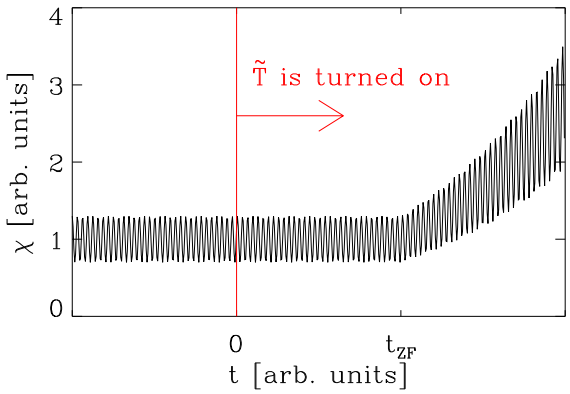

FIG. 4. (Color online) Cartoon of ITG turbulence undergoing an NZT, in terms of the time dependence of the heat diffusivity χ. At $t = 0$, the temperature gradient of the marginal system is increased, leading to an NZT once the zonal flow has decayed sufficiently, at $t = t_{\mathrm{ZF}}$. For simplicity, the turbulence is not affected by the zonal flow decay until the runaway phase.

physics, using this simple heat diffusion model is an intuitive choice—it is straightforward to repeat this calculation for different transport models.

Now, based on the previous assumption that ITG turbulence governs the heat transport throughout the radius, one can use this behavior to predict heat transport in the event that the NZT threshold is crossed locally. Quantitatively, and ignoring quasi-stationary fluctuations, the heat diffusivity at the radial position of the perturbation ψ_{pert} can thus be expressed as

$$\chi(t, \psi_{\mathrm{pert}}) = \chi_0(\psi_{\mathrm{pert}}) \begin{cases} \mathrm{e}^{2\gamma_{\mathrm{ITG}}(\psi_{\mathrm{pert}})\,[t - t_{\mathrm{ZF}}]} & t \geq t_{\mathrm{ZF}} \\ 1 & t < t_{\mathrm{ZF}} \end{cases} . \tag{8}$$

Here, χ_0 denotes the heat diffusivity of the unperturbed system, and $2\gamma_{\mathrm{ITG}}$ is twice the linear ITG growth rate, given that χ is a quantity quadratic in the turbulent amplitude and that the ITG mode undergoes exponential growth during a linear phase in the absence of the zonal flow saturation mechanism.

One can now estimate the time t_{d} necessary for the diffusivity to transport the perturbed heat $\tilde{T}$ away from ψ_{pert}. For $t \geq t_{\mathrm{ZF}}$, heat transport is governed by the modified diffusion equation

$$\frac{\partial (T + \tilde{T})}{\partial t} - \nabla \chi_0 \mathrm{e}^{2\gamma_{\mathrm{ITG}}(t - t_{\mathrm{ZF}})} \cdot \nabla (T + \tilde{T}) = S \, . \tag{9}$$

In order to be able to subtract the unperturbed diffusion equation, the term $\nabla \cdot \chi_0 \nabla T$ is neutrally subtracted and added again. Focusing on only the perturbed part of the heat

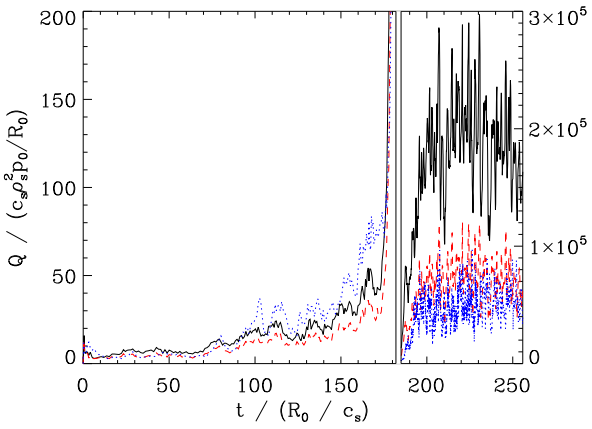

FIG. 5. (Color online) Example of an NZT-unstable simulation at the beginning of the non-zonal phase. Parameters are CBC with $\beta = 1.2\%$. Respectively, the black solid, red dashed, and blue dotted lines denote the ion and electron electrostatic heat fluxes, as well as the electron electromagnetic flux. This serves to illustrate the applicability of the idealized picture shown in Fig. 4: the end of the linear phase around $t = 100$ corresponds to $t = 0$ in the cartoon, whereas t_{ZF} may be placed near $t = 130$. The right side of the plot, with a rescaled y axis, shows the phase of high-flux, second saturation.

transport, this equation reduces to

$$\frac{\partial \tilde{T}}{\partial t} - \nabla\chi_0 \, \mathrm{e}^{2\gamma_{\mathrm{ITG}}(t-t_{\mathrm{ZF}})} \cdot \nabla T + \nabla \cdot \chi_0 \nabla T = 0 \; , \tag{10}$$

where the last term is negligible, as it involves much slower background transport time scales, and therefore

$$\frac{\partial \tilde{T}}{\partial t} - \nabla\chi_0 \, \mathrm{e}^{2\gamma_{\mathrm{ITG}}(t-t_{\mathrm{ZF}})} \cdot \nabla T = 0 \; . \tag{11}$$

Here, the diffusive term is transport of the large, unperturbed temperature by the greatly enhanced diffusivity involving γ_{ITG}. This expression is now integrated over the volume enclosed by A_ψ and over time up to t_{d}, yielding

$$\int \mathrm{d}^3x \, \tilde{T} = \frac{\chi_0}{2\gamma_{\mathrm{ITG}}} \left(\mathrm{e}^{2\gamma_{\mathrm{ITG}}(t_{\mathrm{d}}-t_{\mathrm{ZF}})} - 1 \right) \frac{T}{L_T} A_\psi \; . \tag{12}$$

In the last step, the time integration had a lower integration limit of t_{ZF}, due to the fact that for $t < t_{\mathrm{ZF}}$, the faster non-zonal transport process does not yet act on the temperature profile. Using Eq. (7) to replace χ_0 with q_a and solving for t_{d}, one obtains

$$t_{\mathrm{d}} = t_{\mathrm{ZF}} + \frac{1}{2\gamma_{\mathrm{ITG}}} \ln \left(\frac{n_0 \int \mathrm{d}^3x \, \tilde{T}}{2\gamma_{\mathrm{ITG}} q_a} + 1 \right) \approx t_{\mathrm{ZF}} + \frac{1}{2\gamma_{\mathrm{ITG}}} \ln \left(\frac{n_0 \int \mathrm{d}^3x \, \tilde{T}}{2\gamma_{\mathrm{ITG}} q_a} \right) \; . \tag{13}$$

As the standard ITG turbulence would dissipate a small heat perturbation at a rate of approximately $\tilde{T}/q_a$, this expression combines the regular microturbulent diffusion process with an enhanced rate $\gamma_{\mathrm{ITG}}^{-1}$ in a geometric mean. The disparity of the two scales mixed in this expression makes it possible to drop the second term in the logarithm, by assuming a large-argument expansion. It is important to note that while the argument is large, it may not be so large as to increase t_{d} until it reaches the second saturation phase (see Fig. 5). There tends to be, however, a sufficient time span which satisfies all requirements; in Fig. 5, the simulation achieves second saturation after $t_{\mathrm{d}} \gg \gamma_{\mathrm{ITG}}^{-1}$, underscoring the applicability of this approach.

Since both t_{ZF} and $\gamma_{\mathrm{ITG}}^{-1}$ are very small compared with $\tilde{T}/q_a$, NZT-aided dissipation of a heat blob occurs on extremely fast time scales. Therefore, heating a system to the point where it is NZT-unstable for longer periods of time is not feasible—instead, $\beta_{\mathrm{crit}}^{\mathrm{NZT}}$ can be expected to constitute an extremely stiff limit (which can alternatively be interpreted as a limit on the pressure gradient).

IV. SUMMARY

The quantities central to field line decorrelation – and, by extension, to the physics underlying the non-zonal transition – are the half-turn displacement $\Delta r_{1/2}$ and the correlation length λ_{Bxx}. Using a database of gyrokinetic turbulence simulations, as well as matching with previous analyses, $\Delta r_{1/2}$ has been expressed as a function of β and the heat diffusivity χ_{eff}, whereas λ_{Bxx} was found to vary weakly and was thus replaced by its database average. With these manipulations, a simple rule was derived at which $\beta_{\mathrm{crit}}^{\mathrm{NZT}}/\beta_{\mathrm{crit}}^{\mathrm{KBM}} \approx 8.6/(q_0\chi_{\mathrm{eff}}^{1/2})$ one may expect an NZT to occur.

In a separate effort, the transport properties of a system were investigated which is marginally stable, $\beta = \beta_{\mathrm{crit}}^{\mathrm{NZT}}$. When perturbed through the imposition of a heat blob $\tilde{T} \ll T$, it was found that said heat blob is diffusively transported on a time scale much faster than the usual transport time, namely one that involves the linear growth time of the ITG instability. Therefore, it is concluded that, given certain conditions are met, the NZT may provide a very efficient transport channel which makes it all but impossible to operate a fusion experiment well within an NZT regime. Instead, $\beta_{\mathrm{crit}}^{\mathrm{NZT}}$ sets a strict operational limit.

ACKNOWLEDGMENTS

W.M. Nevins, F. Jenko, T. Görler, and D. Told have made essential contributions to the research focused on the non-zonal transition—for which the authors are deeply grateful.

---

[1] M.J. Pueschel, P.W. Terry, F. Jenko, D.R. Hatch, W.M. Nevins, T. Görler, and D. Told, Phys. Rev. Lett. **110**, 155005 (2013)

[2] M.J. Pueschel, D.R. Hatch, T. Görler, W.M. Nevins, F. Jenko, P.W. Terry, and D. Told, Phys. Plasmas **20**, 102301 (2013)

[3] W.M. Nevins, E. Wang, I. Joseph, J. Candy, S.E. Parker, Y. Chen, and G. Rewoldt, *Turbulence-Driven Magnetic Reconnection*, American Physical Society, 51st Annual Meeting of the APS Division of Plasma Physics (2009)

[4] R.E. Waltz, Phys. Plasmas **17**, 072501 (2010)

[5] M.N. Rosenbluth and F.L. Hinton, Phys. Rev. Lett. **80**, 724 (1998)

[6] W.M. Nevins, J. Candy, S. Cowley, T. Dannert, A. Dimits, W. Dorland, C. Estrada-Mila, G.W. Hammett, F. Jenko, M.J. Pueschel, and D.E. Shumaker, Phys. Plasmas **13**, 122306 (2006)

[7] M.J. Pueschel, T. Görler, F. Jenko, D.R. Hatch, and A.J. Cianciara, Phys. Plasmas **20**, 102308 (2013)

[8] P.W. Terry, M.J. Pueschel, D. Carmody, and W.M. Nevins, Phys. Plasmas **20**, 112502 (2013)

[9] E. Wang, W.M. Nevins, J. Candy, D. Hatch, P. Terry, and W. Guttenfelder, Phys. Plasmas **18**, 056111 (2011)

[10] M.J. Pueschel, F. Jenko, M. Schneller, S. Günter, and G. Tardini, Nucl. Fusion **52**, 103018 (2012)

[11] R.E. Waltz, Phys. Fluids **28**, 577 (1985)

[12] A.M. Dimits, G. Bateman, M.A. Beer, B.I. Cohen, W. Dorland, G.W. Hammett, C. Kim, J.E. Kinsey, M. Kotschenreuther, A.H. Kritz, L.L. Lao, J. Mandrekas, W.M. Nevins, S.E. Parker, A.J. Redd, D.E. Shumaker, R. Sydora, and J. Weiland, Phys. Plasmas **7**, 969 (2000)

[13] M.J. Pueschel and F. Jenko, Phys. Plasmas **17**, 062307 (2010)

[14] H. Biglari, P.H. Diamond, and M.N. Rosenbluth, Phys. Fluids B, **1**, 109 (1989)

[15] F. Romanelli and S. Briguglio, Phys. Fluids B, **2**, 754 (1990)